Kr, He, N_2, and D_2 adsorbed on graphite[20-22] and the $\alpha \rightleftarrows \beta$ transition studied in O_2 adsorbed on the same substrate.[22] The first one is induced by potential wells of the substrate surface, the second one is due to magnetic ordering. For NO adsorbed on graphite, the size and the shape of dimers are important parameters in the stabilization of 2D solids.

We are especially grateful to P. Thorel and J. G. Dash for numerous fruitful discussions and the D1B staff for helping us in the neutron measurements in Grenoble.

[a]Permanent address: Laboratoire M. Letort, 54600 Villers-les-Nancy, France.

[b]Permanent adress: Institut Laue-Langevin, B. P. 156, 38042 Grenoble, France.

[1]R. E. Peierls, Ann. Inst. Henri Poincaré 5, 1771 (1935).

[2]L. Landau, Phys. Z. Sowjetunion 11, 26 (1937).

[3]N. D. Mermin, Phys. Rev. 176, 250 (1968).

[4]J. M. Kosterlitz and D. J. Thouless, J. Phys. C 6, 1181 (1973).

[5]Y. Imry and L. Gunther, Phys. Rev. B 3, 3939 (1971).

[6]J. G. Dash, *Films on Solid Surfaces* (Academic, New York, 1975).

[7]M. Bretz, J. G. Dash, D. C. Hickernell, E. O. McLean, and O. E. Vilches, Phys. Rev. A 8, 1589 (1973).

[8]G. B. Huff and J. G. Dash, J. Low Temp. Phys. 24, 155 (1976).

[9]T. T. Chung and J. G. Dash, Surf. Sci. 66, 559 (1977).

[10]H. Shechter, J. Suzanne, and J. G. Dash, Phys. Rev. Lett. 37, 706 (1976).

[11]J. K. Kjems, L. Passell, H. Taub, J. G. Dash, and A. D. Novaco, Phys. Rev. B 13, 1446 (1976).

[12]H. Taub, K. Carneiro, J. K. Kjems, L. Passell, and J. P. McTague, Phys. Rev. B. 16, 4551 (1977).

[13]J. P. Coulomb, M. Bienfait, and P. Thorel, J. Phys. (Paris), Colloq. 38, C4-31 (1977).

[14]R. J. Rollefson, Phys. Rev. Lett. 29, 410 (1972).

[15]B. P. Cowan, M. G. Richards, A. L. Thomson, and W. J. Mullin, Phys. Rev. Lett. 38, 165 (1977).

[16]M. Matecki, A. Thomy, and X. Duval, J. Chim. Phys. 71, 1484 (1974), and to be published.

[17]Papyex is a recompressed exfoliated graphite from Le Carbone Lorraine and is very similar to Grafoil marketed by Union Carbide (Ref. 6).

[18]R. W. G. Wyckoff, *Crystal Structures* (Wiley, London, 1963), Vol. 1.

[19]*International Tables for X-Ray Crystallography* (The Kynoch Press, Birmingham, 1965).

[20]J. A. Venables, H. M. Kramer, and G. L. Price, Surf. Sci. 55, 373 (1976).

[21]S. C. Fain, Jr., and M. D. Chinn, J. Phys. (Paris), Colloq. 38, C4-99 (1977).

[22]M. Nielsen, J. P. McTague, and W. Ellenson, J. Phys. (Paris), Colloq. 38, C4-10 (1977).

Charge Distribution in *c* Direction in Lamellar Graphite Acceptor Intercalation Compounds

L. Pietronero, S. Strässler, and H. R. Zeller
Brown Boveri Research Center, CH-5401 Baden, Switzerland

and

M. J. Rice
Xerox Webster Research Center, Webster, New York 14580

(Received 25 August 1977)

We calculate the charge distribution $\rho(z)$ and Fermi-level distribution among the different graphite layers in a lamellar graphite acceptor compound. The charge distribution is highly nonhomogeneous and, because of the semimetallic nature of graphite, nonlinear effects are important. The calculations for $\rho(z)$ are performed in terms of a generalized Thomas-Fermi model and show that there is a transition at short distances from the intercalate from a z^{-4} power law to an exponential asymptotic decay.

The long-standing interest[1] in graphite intercalation compounds has been considerably enhanced by recent reports[2,3] of electrical conductivities exceeding that of copper in some of these compounds. Nevertheless, important questions concerning the electronic structure of such compounds are not settled yet. It is the purpose of this paper to clarify one important point, viz., the charge distribution in the *c* direction.

Lamellar graphite intercalation compounds form ordered sequences of graphite and intercalate layers characterized by the stage *n* where *n* denotes the number of graphite layers between two successive intercalate layers. It is generally agreed that the intercalate ions act as donors or acceptors transferring electrons or holes, re-

spectively, to the graphite. The charge transfer is expressed in terms of a parameter f which denotes the fractional electronic charge transferred per intercalate ion. There is a considerable amount of disagreement on the value of f even in the carefully studied graphite halogen compounds. Typically, transport experiments indicate a high degree of ionization ($0.1 \lesssim f \lesssim 1$) whereas experiments which directly probe the Fermi surface result in a small value of f.[4] The f values given in Ref. 4 have been deduced under the assumption that the charge transfer results in a homogeneous shift of the graphite Fermi level or, in other words, in a homogeneous charge distribution $\rho(z)$ in the z direction.

The screening length in a standard metal is of order of 1 Å. For graphite, because of its much smaller carrier concentration, a larger value is expected but there is no *a priori* basis for the assumption[5] that the screening length is large compared to the intercalate layer separation in dilute compounds.

Spain and Nagel[6] have estimated a screening length of about 5 Å in pure graphite. In intercalation compounds the strong Fermi-energy dependence of the carrier concentration leads to a pronounced nonlinearity and the breakdown of the concept of a screening length. We introduce a generalized Thomas-Fermi model to deal with screening in semimetals in general and apply it to graphite intercalation compounds.

The interaction between intercalate and graphite is in general much more complex than the simple charge-transfer model suggests. Girifalco and Holzwarth[7] have calculated the electron density in a stage-1 LiC_6 compound and have discussed the deviations from a simple-minded ionic model. We note, however, that all interactions except the electrostatic are short range and thus restricted to the layers adjacent to the intercalate (bounding layers). In this paper we are exclusively interested in the screening of the electrical field induced by the intercalate. We avoid all problems associated with short-range interactions in the first layer by defining an effective f which produces the correct long-range fields and treating it as a free parameter. Furthermore we restrict the calculation to acceptor compounds in which covalency effects are less important as is evident from their large anisotropy in electrical conductivity.

Our calculation is based on the Thomas-Fermi model which assumes a local relation between charge and electrostatic potential. The Thomas-Fermi model can be characterized as the $q \to 0$ limit of the Lindhard screening model[8] and its accuracy increases with decreasing carrier concentration, i.e., increasing screening length. We thus expect it to be a very good appoximation for graphite intercalation compounds. Furthermore we treat the problem as one dimensional, i.e., we assume the charge to be homogeneously distributed perpendicular to the c direction.

We consider a stage-n lamellar compound. $\rho(z)$ denotes the charge distribution in the c direction, $\mu(z)$ the Fermi energy, and $E(z)$ the electrical field in the graphite layers induced by $\rho(z)$ and the charged intercalate. Poisson's equation reads

$$\frac{dE(z)}{dz} = \frac{4\pi}{\epsilon_\perp}\rho(z) = \frac{4\pi e}{\epsilon_\perp}[p(\mu_z) - n(\mu_z)]. \quad (1)$$

Here $\epsilon_\perp$ denotes the dielectric constant in the c direction, $\mu_z = \mu(z)$, and p and n are the concentrations of holes and electrons, respectively. For small μ, $n(\mu)$ and $p(\mu)$ are markedly temperature dependent.

The equilibrium condition for the Fermi level $\mu(z)$ is, within the Thomas-Fermi approximation,

$$d\mu(z)/dz = E(z). \quad (2)$$

By combining (1) and (2) we obtain

$$d^2\mu(z)/dz^2 = (4\pi e/\epsilon_\perp)[p(\mu_z) - n(\mu_z)]. \quad (3)$$

For simple forms of $p(\mu) - n(\mu)$, Eq. (3) can be solved analytically. If the total density of states is constant $N(\mu) = N_0$, then

$$d^2\mu(z)/dz^2 = (4\pi e/\epsilon_\perp)N_0[\mu(z) - \mu_0] \quad (4)$$

and both $\mu(z)$ and $\rho(z)$ vary exponentially with a screening length

$$\lambda = (\epsilon_\perp/4\pi e N_0)^{1/2}.$$

For semimetals or zero-gap semiconductors the density of states can sometimes be approximated by a power law $N(\mu) \sim (\mu - \mu_0)^\alpha$. In this case Eq. (3) becomes

$$d^2\mu(z)/dz^2 \sim [\mu(z) - \mu_0]^{\alpha+1}. \quad (5)$$

Equation (5) can be solved analytically and we find $\mu(z)$ and $\rho(z)$ to be power laws with powers $-2/\alpha$ and $-2(\alpha+1)/\alpha$, respectively. For large shifts of the Fermi level in graphite, $N(\mu)$ is approximately linear in μ and by solving (5) with the appropriate boundary conditions for an infinitely dilute compound we obtain

$$\rho(z) \sim (1 + z/z_0)^{-4}, \quad \mu(z) - \mu_0 \sim (1 + z/z_0)^{-2}, \quad (6)$$

where $z = 0$ is located at the intercalate-graphite

interface and $z_0 \sim f^{-1/3}$.

In general $N(\mu)$ has to be computed from the band structure and (3) has to be solved numerically. Since (3) is nonlinear, several solutions may exist of which the one with the minimum total (band plus electrostatic) energy is physically relevant.

To calculate $\rho(z)$ and $\mu(z)$ based on Eq. (3) we have to know the carrier density $p(\mu) - n(\mu)$ as a function of Fermi energy for graphite. We have computed $p(\mu) - n(\mu)$ from the Slonczewsky-Weiss-McClure[9] band model using the same band parameters as in (5).

Before we can solve Eq. (3) we have to specify $\epsilon_\perp$ which represents the dielectric constant in the c direction and includes all contributions except free carriers. $\epsilon_\perp$ thus has to be deduced from far-infrared studies and is found[10] to be $\epsilon_\perp = 5.4$.

The experimental situation with regard to the exact value of $\epsilon_\perp$ is not clear[10] and we note that in the power-law regime [Eq. (6)] the characteristic length z_0 varies as $\epsilon_\perp^{2/3}$ and in the asymptotic linear regime the screening length λ varies as $\epsilon_\perp^{1/2}$. A smaller $\epsilon_\perp$ would thus decrease the screening distances and enhance the nonlinearity.

For the following calculations it is most convenient to take $z = 0$ at the center of the n graphite layers. The two layers bounding the intercalate are then located at $z = \pm(n-1)c/4$ where $c = 6.74$ Å is twice the layer spacing of pure graphite. For symmetry reasons $\partial\rho(0)/\partial z = \partial\mu(0)/\partial z = 0$ and $\mu(0)$ is a free parameter which for each value of n defines f.

We have numerically calculated the charge distribution $\rho(z)$ and Fermi-level distribution $\mu(z)$ for acceptor lamellar compounds based on the formalism discussed above. First we discuss the extremely dilute limit ($n \gtrsim 30$). This limit is characterized by a virtually unperturbed region of graphite around $z = 0$ and thus in the vicinity of the intercalate $\rho(z)$ does not depend on n.

In Fig. 1 we have plotted ρ and $\Delta\mu$ as a function of distance from the intercalate layer in the extremely dilute limit for different values of f. In this calculation f refers to an AC_{6n} compound. Other stoichiometries are covered by redefining f ($f = 1$ for AC_{8n} corresponds to $f = 0.75$ for AC_{6n}, etc.). For small distances and $f = 1$, ρ varies according to the power law of Eq. (6) with $z_0 \sim 5.2$ Å. The analytical solution of Eq. (5) assuming a linear density-of-states dispersion $N(\mu)$ yields $z_0 = 5.4$ Å. For small f or large distances, the asymptotic decay of ρ is exponential with a screening length of 7.7 Å. The nonlinearity is also evident from Table I. The fraction of transferred charge localized in the bounding layers markedly depends on f whereas the distance l_K at which the Fermi surface crosses the conduction-band extremum at the K point depends less on f than expected from a linear model.

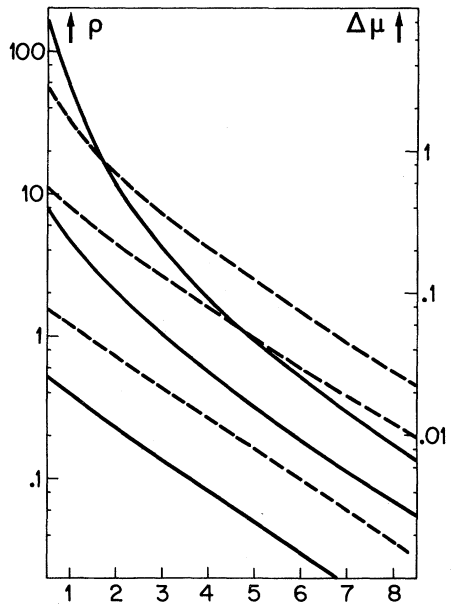

FIG. 1. Charge density ρ (solid line) in units of 10^{20} cm^{-3} and shift in chemical potential $\Delta\mu$ (dashed line) in eV as a function of distance from the intercalate-graphite interface. The abscissa is in units of graphite layer spacings and the three curves in decreasing magnitude refer to f values of 1, 0.1, and 0.01, respectively. All values are given for an AC_{6n} compound at $T = 0$ in the extremely dilute limit.

We now discuss somewhat more concentrated compounds. Obviously a critical stage n_K or concentration c_K is reached when the electron pocket of the Fermi surface disappears in the center graphite layer at $z = 0$, i.e., the Fermi surface crosses the K-point conduction-band extremum. For an AC_{6n} compound, for $f = 1$, 0.1, 0.01, we find $n_K = 20$, 17, 10 and $c_K = 0.83$, 0.98, and 1.66 at.% respectively. These numbers should be compared with results from Shubnikov–de Haas[11] and magnetoreflection[12,13] experiments. Chung and Dresselhaus[12] and Platts, Chung, and Dresselhaus[13] have carried out careful magnetoreflection experiments on graphite-Br_2 residue compounds. They were able to label the observed transitions according to the band structure of pure graphite. With increasing Br_2 concentration the observed signals decrease in intensity but the oscillation periods re-

TABLE I. f dependence of screening parameters in the extremely dilute limit. The indicated f values correspond to an AC_{6n} compound, i.e., $f=1$ corresponds to a two-dimensional charge density of 6.4×10^{14} e/cm^2 in an intercalate layer. ρ_1 is the fraction of transferred charge localized in the two bounding graphite layers and l_K is the distance at which the Fermi surface crosses the K-point conduction-band extremum. All values are calculated for $T=0$.

f	ρ_1	l_K (Å)
1	0.77	29.2
0.3	0.64	26.5
0.1	0.53	22.8
0.03	0.44	17.1
0.01	0.41	10.5
$\rightarrow 0$	0.35	...

main virtually unchanged. From the cutoff of a particular resonance transition it is found that the Fermi surface crosses the K point at a Br_2 contration of about 0.6 at.%. The results were interpreted under the assumption of a homogeneous shift of the Fermi level and it was concluded that $f\sim0.02$. On the basis of our calculation we would argue that cutoff occurs when the Fermi level of the layers at $z\sim0$ cross the K-point extremum, i.e., at a Br_2 concentration c_K which depends on f. Since the experiments have been carried out on residue compounds in which the intercalate is associated with defects and not stacked in a regular way it is impossible to make a quantitative contact to our calculation. We note two things, however: The observed cutoff concentration is close to the range calculated for lamellar compounds and the calculated c_K's depend very little on f. Since the distribution of intercalate ions in the specimens of Refs. 12 and 13 is not known, the magnetoreflection results have to be considered consistent with virtually any value $0<f<1$. This example serves to illustrate the importance of a realistic $\rho(z)$ for a correct interpretation of experimental results.

Next we discuss the charge distribution in concentrated compounds. Since we are interested in the charge distribution among the graphite layers and not within one layer, the cases $n=1, 2$ are trival by symmetry. In a stage-3 compound the fractional distribution among the three layers can be characterized by a parameter x_3 such that the distribution becomes $(1-x_3)/2$, x_3, $(1-x_3)/2$. In a stage-4 compound x_4 is analogously defined by $(1-2x_4)/2$, x_4, x_4, $(1-2x_4)/2$. A homogeneous distribution corresponds to $x_3=\frac{1}{3}$ and $x_4=\frac{1}{4}$. Table II gives values of x_3, x_4 for different f's corresponding to an AC_{6n} compound. (With decreasing f the charge distribution becomes more homogeneous.)

TABLE II. Charge distribution in state-2 $(1-x_3)/2$, x_3, $(1-x_3)/2$ and stage-4 $(1-2x_4)/2$, x_4, x_4, $(1-2x_4)/2$ compounds for different values of f (f defined for an AC_{6n} compound). The last entry gives the asymptotic value for $f\rightarrow0$.

f	x_3	x_4
1	0.16	0.10
0.3	0.21	0.14
0.1	0.26	0.18
0.03	0.29	0.20
0.01	0.30	0.21
$\rightarrow0$	0.31	0.23

One may argue that the results of a Thomas-Fermi calculation become questionable if $\rho(z)$ shows rapid variation within one graphite layer. Figure 1 shows that $\rho(z)$ varies rapidly within the first layer for $f\sim1$. In the framework of a tight-binding rigid-band model, $\rho(z)=\mathrm{const}$ for each graphite layer. We have thus repeated the calculation of x_3 and x_4 for $f=1$ assuming $\rho(z)=\mathrm{const}$ within each layer. The results agree very well with the values given in Table II showing that the overall behavior of $\rho(z)$ does not depend on the details of the charge distribution within each layer. However, the calculations show this to hold only for not too large f's; for hypothetical f values $f\gtrsim3$, x_3 and x_4 would become strongly dependent on the detailed distribution.

We have shown that because of the small number of free carriers in pure graphite and the pronounced dependence of carrier concentration on Fermi energy, the screening of the intercalate charge density is complex. The high carrier density associated with large shifts of Fermi energy provides an effective screening in the vicinity of the intercalate but the small carrier density of pure graphite leads to a relatively long tail in dilute compounds. In general, experiments on intercalation compounds have been interpreted either by assuming $\mu(z)=\mathrm{const}$ throughout the graphite (see, for instance Ref. 5) or by assuming $\mu(z)=\mathrm{const}$ in the layers not bounding the intercalate (see, for instance Ref. 6). Our calculations show both models to be inadequate and give for the first time a realistic $\mu(z)$ and $\rho(z)$

which has to form the basis for a correct interpretation of experimental results on transport, optical, and Fermi-surface experiments.

It is a pleasure to thank Dr. W. Schneider and Dr. H. J. Wiesmann for useful discussions and Professor A. R. Ubbelohde, F.R.S., for interesting suggestions and comments in the final stage of our work.

[1]G. R. Henning, Prog. Inorg. Chem. 1, 125 (1959); A. R. Ubbelohde and L. A. Lewis, *Graphite and Its Crystal Compounds* (Oxford Univ. Press, Oxford, 1969).

[2]F. L. Vogel, Bull. Am. Phys. Soc. 21, 262 (1978).

[3]*Intercalation Compounds of Graphite*, edited by F. L. Vogel and A. Hérold (Elsevier Sequoia, Lausanne, 1977).

[4]For a review and discussion see paper by G. Dresselhaus and M. S. Dresselhaus, in Ref. 3.

[5]M. S. Dresselhaus, G. Dresselhaus, and J. E. Fisher, Phys. Rev. B 15, 3180 (1977).

[6]I. L. Spain and D. J. Nagle, in Ref. 3.

[7]L. A. Girifalco and N. A. W. Holzwarth, in Ref. 3.

[8]C. Kittel, *Quantum Theory of Solids* (Wiley, New York, 1963).

[9]J. W. McClure, Phys. Rev. 108, 612 (1957); J. C. Slonczewski and P. R. Weiss, Phys. Rev. 109, 272 (1958).

[10]H. Venghaus, Phys. Status Solidi 81, 221 (1977).

[11]A. S. Bender and D. A. Young, J. Phys. C 5, 2163 (1972).

[12]D. D. L. Chung and M. S. Dresselhaus, Solid State Commun. 19, 227 (1976).

[13]D. A. Platts, D. D. L. Chung, and M. S. Dresselhaus, Phys. Rev. B 15, 1087 (1977).

Magnetization Reversal of a FeSi Picture-Frame Crystal Measured by the Time-Dependent Neutron-Depolarization Technique

F. J. van Schaik and M. Th. Rekveldt
Interuniversitair Reactor Instituut, Delft, The Netherlands
(Received 23 June 1978)

The magnetization-reversal process within a [100] [010] [001] picture-frame FeSi (3.5 wt% Si) crystal has been investigated by means of the time-dependent neutron-depolarization technique, applying a periodic block-shaped magnetic field. Various distinct states are observed in the magnetization-reversal process: firstly, nucleation of regions of reversed magnetization; subsequently, the merging of these regions into two wavy domain walls according to a sandwich structure and the motion of these straightening walls towards the center.

It has long been recognized that magnetization reversal in a ferromagnet under the influence of a pulsed magnetic field can be described in terms of nucleation regions of reversed magnetization (denoted reversed regions) and eddy-current–controlled domain-wall motion.[1,2] However, the experimental information about the reversal process is restricted by the detection techniques used up to now: pickup coils to measure the average magnetization of the bulk material combined with Kerr-effect observations of the surface behavior of the domain walls. In contrast, polarized neutrons are a unique probe for investigating magnetic domains within the volume of a ferromagnet.[3,4] Time-dependent neutron-depolarization technique[5,6] (TDNDT) gives information with a spatial resolution of several microns about the internal magnetization distribution and the local direction of the magnetization. In this Letter we report the results of applying the newly developed TDNDT to study the magnetic reversal processes within a single-crystal picture-frame specimen of silicon(3.5 wt%) iron.

In the neutron-depolarization technique[4] the polarization direction of a monochromatic neutron beam impinging in the x direction on the sample can be adjusted before and analyzed after transmission along any of the three orthogonal directions x, y, and z (Fig. 1). The polarization change D_{ij} by the sample is defined by $D_{ij}=(I_s-I_{ij})/(I_s-I_0)$, in which I_s is the intensity of a fully depolarized beam, I_{ij} the intensity with analyzation and polarization directions i and j ($i, j=x, y, z$), and I_0 the intensity of the undisturbed polarized beam.

The polarization direction of the neutron beam rotates with the Larmor precession frequency around the magnetization direction in the crystal. The total rotation angle ϕ is given by $\phi=\gamma B_s d/v$, where γ is the gyromagnetic ratio of the neutron ($\gamma=1.80\times10^8$ s^{-1} T^{-1}, mksa units), B_s the spontaneous magnetic induction, v the velocity of the neutrons, and d the crystal thickness. The length $|D|$ and rotation angle ϕ of the polarization vector

